

# Impact of DSSCs structure modification sensitized with phenothiazine derivative on photovoltaic performance

Paweł Gnida<sup>1\*</sup>, Aneta Słodek<sup>2</sup>, Mieczysław Łapkowski<sup>1,3,4</sup>, Ewa Schab-Balcerzak<sup>1,2</sup>

<sup>1</sup> Centre of Polymer and Carbon Materials, Polish Academy of Sciences, 34 M. Curie-Skłodowskiej Str., 41-819 Zabrze, Poland

<sup>2</sup> Institute of Chemistry, University of Silesia, 9 Szkolna Str., 40-006 Katowice, Poland

<sup>3</sup> Faculty of Chemistry, Silesian University of Technology, 9 M. Strzody Str., 44-100 Gliwice, Poland

<sup>4</sup> Centre for Organic and Nanohybrid Electronics, Silesian University of Technology, 22b Konarskiego Str., 44-100 Gliwice, Poland

## Article info

### Article history:

Received 04 Aug. 2024

Received in revised form 09 Oct. 2024

Accepted 14 Oct 2024

Available on-line 08 Nov. 2024

### Keywords:

dye-sensitized solar cell;

N719;

organic dyes;

phenothiazine derivatives;

co-sensitization.

## Abstract

This paper presents the results of a study on the modification of dye-sensitized solar cells (DSSCs) using various phenothiazine derivatives, N719, and a mixture of these. The influence of the solvent used to prepare the dye solution, as well as the use of a TiO<sub>2</sub> blocking layer, the addition of a co-adsorbent, or a mixture of dyes with N719 are presented. Characterisation of photoanodes was carried out to determine the UV-Vis absorption properties, morphology, and photovoltaic parameters of the fabricated solar cells. The use of different solvents for the preparation of dye solutions resulted in DSSCs efficiencies in the range of 1.55–7.26%. The most advantageous was using an ACN:t-BuOH mixture, which provided the best efficiency. The application of further modifications in the form of the addition of chenodeoxycholic acid (CDCA), a blocking layer, and the use of a co-sensitization process resulted in an increase in the final efficiency to a value of 8.50%.

## 1. Introduction

Photovoltaics (PV) is one of the most promising technologies for obtaining energy from renewable sources. Solar cells are now being used on a large scale in the industry by covering roofs and open spaces with PV panels, thus reducing energy consumption generated from non-renewable sources. They are also used in smaller forms, such as household power plants, to generate electricity for single households [1, 2]. Among various development paths in PV, the direction associated with dye-sensitized solar cells (DSSCs) is noteworthy. Currently, record efficiencies of DSSC devices exceed 14% [3, 4]. The main advantages of DSSCs include their ability to operate at wide incident angles and low irradiance, their capability to change colour and transparency, and their relatively uncomplicated fabrication methods [5–7]. To improve the performance of DSSC devices, various methods are employed, such as using blocking layers (BL), scattering layers (SL), and adding nanoparticles (e.g., TiO<sub>2</sub>) [8–13]. BL are widely used and intensively researched. Researchers primarily focus on selecting the appropriate material, layer thickness, and preparation method, which

ultimately determines the properties of the obtained layer. These BL are most often made of oxide materials such as TiO<sub>2</sub>, ZnO, Al<sub>2</sub>O<sub>3</sub>, SiO<sub>2</sub>, SnO<sub>2</sub> or ZrO<sub>2</sub> [14–17]. Sometimes using BL can increase the amount of adsorbed dye molecules [18, 19]. Another modification is using a co-adsorbent to prevent dye aggregation by anchoring to TiO<sub>2</sub> and separating dye molecules from each other. Cholic acid (CA), deoxycholic acid (DCA) and chenodeoxycholic acid (CDCA) are the most commonly used co-adsorbents [20–23]. New metal-free dyes are being sought to improve the performance of the cells and reduce the cost of preparing the device. Phenothiazine derivatives are particularly noteworthy due to their non-planar conformation which can significantly reduce dye aggregation during anchoring to the oxide substrate and prevent excimer formation. Additionally, they contain electron-rich sulphur and nitrogen heteroatoms in their structure which enhances their donor properties [24–26]. Having the dyes used in DSSCs to achieve high PV performance, it is also worth considering using them together with, for example, N719. The concept of using a mixture (co-sensitization) of dyes should also be noted. Firstly, this allows a significant increase in the absorption range of incident light. Furthermore, if mixed with an N719 dye, half as much expensive commercial dye is used compared to a solar cell containing

\*Corresponding author at: [pgnida@cmpw-pan.pl](mailto:pgnida@cmpw-pan.pl)

only the N719 dye. In the vast majority of cases, using a dye mixture leads to higher efficiency than with single dyes [27–31]. In Ref. 27, single solar cells containing either N719 or D-1 (bitiophene derivative) dye was described which had efficiencies of 5.75% and 0.14%, respectively. The cell containing a mixture of these two dyes had higher efficiencies of up to 6.30%. Reference 28 describes the use of co-sensitization of an N719 dye and a phenothiazine derivative and the fabrication of a DSSC with such an arrangement which had a power conversion efficiency of 8.12% while for single dyes, the cells showed efficiencies of 6.97% and 5.81%, respectively. Wang *et al.* [29] described the use of a mixture of two dyes, including N719 and diphenylpyranilidene dye and the effect of the addition of CDCA as a co-adsorbent. Using co-sensitization process, it was possible to improve device efficiency to 8.20% from 7.77% (N719) and 4.77% for a cell containing a second dye. The addition of CDCA resulted in a further increase in power conversion efficiency to 8.49% (10 mM CDCA). In Ref. 30, a literature review was carried out to show the essence of the application of the co-sensitization process using up to three dyes with complementary absorption spectra, dramatically increasing the photoanode absorption range. Job *et al.* described [31] a study of the stability of DSSCs containing a dye mixture over time at different incident light intensities. For this purpose, a series of solar cells containing anchored dye molecules N719 and a TPA derivative were prepared. Very interesting results were obtained, the highest efficiency was 6.44% at a  $108 \text{ mW cm}^{-2}$  illumination intensity after a time period of 100 h, and then a linear decrease started.

The studies focused on the use of dyes that are phenothiazine derivatives. Additionally, experiments were conducted using different solvents [(chloroform, *N,N*-dimethylformamide (DMF) and a mixture of acetonitrile and tert-butanol (1:1)] to fabricate the photoanode. The effects of the dye structure and the type of solvent used on the photoanode properties and PV performance of the fabricated DSSCs were determined. The next stage of the work carried out was to select the best dye from those tested and modify the photoanode by applying a BL, a mixture of dye with N719, and the addition of a co-adsorbent. This paper presents a series of phenothiazine derivatives that have been used in dye cells as light absorbers. In addition to already published results, this time the solvent effect on the cells PV performance was determined, which made it possible to determine the trend of the described changes. Huge changes in efficiency were observed for cells containing the same dye with different solvents, reaching up to more than four percentage points. In addition, a dye was selected that ensured the highest PV performance of the device and, in addition, the structure of the solar cell was modified to further improve the performance, resulting in a power conversion efficiency (PCE) of 8.50%

## 2. Materials and methods

### 2.1. Preparation of $\text{TiO}_2$ mesoporous layers on FTO-coated glass substrates

Glass substrates covered with a layer of fluorine-doped tin oxide (FTO, Sigma Aldrich) were washed. The thickness of FTO was about 500 nm. First, the slides were

placed in a beaker with a 10% aqueous solution of surfactant (Hellamanex) and placed in an ultrasonic bath for 15 min at 40 °C. The substrates were then placed in a beaker containing distilled water and again placed in an ultrasonic bath for 15 min at 40 °C. This step was repeated twice. After this time, the slides were placed in a beaker containing isopropanol and again placed in an ultrasonic bath for 5 min at 40 °C. After the removal from the isopropyl alcohol (IPA), the substrates were allowed to air dry. Layers of  $\text{TiO}_2$ -containing paste (18NR-T, Greatcell Solar Materials) were applied to dry FTO slides using a screen printer. Three layers of paste were applied. Each time after applying a layer, the substrate was annealed for 5 min at 125 °C. After the last layer of  $\text{TiO}_2$  paste was applied and annealed, it was followed by firing in an oven at 500 °C for 30 min. FTO substrates so prepared with an applied  $\text{TiO}_2$  layer were left to cool.

### 2.2. Preparation of the $\text{TiO}_2$ BL

The first step was to prepare a 2 M solution of titanium(IV) tetrachloride from a commercial concentrated aqueous solution of titanium(IV) tetrachloride. The cleaned FTO substrates were then placed in a Petri dish in which 48.75 ml of deionized water was placed and 1.25 ml of 2 M solution of  $\text{TiCl}_4$  was added, obtaining a solution of 0.05 M. The substrates immersed in the solution were heated at 70 °C for 30 min. After this time, the glass substrates were removed from the solution gently rinsed with distilled water, and placed in the oven for 30 min at 500 °C.

### 2.3. Preparation of the photoanodes

Previously prepared FTO glass substrates with a  $\text{TiO}_2$  layer were heated to 80 °C and immersed in a dye solution of  $3 \cdot 10^{-4}$  M for 24 h. Dye N719 was purchased from Greatcell Solar Materials, the synthesis of phenothiazine derivatives was described in literature [10, 32–34]. After this time, the photoanodes were removed from the solution, and the excess dye was removed using ethanol. The photoanodes were left in air to dry. Solvents such as chloroform, DMF and a mixture of acetonitrile and tert-butanol (1:1) (Sigma Aldrich) were used to prepare the dye solution.

### 2.4. Preparation of DSSC devices

The DSSC was constructed by assembling a previously prepared photoanode with a counter-electrode and the space between them was filled with a commercial EL-HSE liquid electrolyte containing  $\text{I}^-/\text{I}_3^-$  ions.

### 2.5. Measurements

A Keithley 2400 SourceMeter source-measuring device (Tektronix, Inc., Beaverton, OR) and software were used to measure the current-voltage characteristics, along with a PV Solutions sunlight simulator giving a standard light output of  $100 \text{ mWcm}^{-2}$  under 1.5 G AM conditions. BL thicknesses and root mean square (RMS) were determined using an atomic force microscope (AFM) TopoMetrix Explorer operating in contact mode in an air atmosphere.

UV-Vis spectra were recorded using a Jasco-V-570 UV-Vis-NIR spectrophotometer.

### 3. Results and discussions

In the first step of the ongoing research, eight phenothiazine derivatives were considered. Each compound contained one anchor group (a cyanoacrylic acid group) in position 3 and an octyl chain in the 10H position. The synthesis of the dyes and their potential application in DSSC cells are described in the following papers – Refs. 10 and 32–34. The chemical structure of the phenothiazine derivatives in question is shown in Fig. 1.

#### 3.1. Optical properties.

Regarding potential application, firstly, the UV-Vis absorption properties of dyes tested in solution were determined using different solvents [chloroform, *N,N*-dimethylformamide and mixtures of acetonitrile and tert-butanol (1:1)], as well as the prepared photoanodes after a 24 h immersion in a solution of the dye in question. For comparative purposes, dye N719 was also tested (if its solubility allowed). Absorption properties of the prepared photoanodes were determined. For all phenothiazine derivatives, only a DMF solution was prepared, as this was the only solvent that provided very good solubility. For selected dyes **PTZ-1**–**PTZ-5** and **PTZ-1**–**PTZ-6**, the absorption properties were determined in chloroform and in an ACN:*t*-BuOH mixture, respectively. Figure 2 shows the selected absorption spectra of photoanodes in the UV-Vis range.

Due to the application, the main focus was on the absorption properties of the photoanodes, first comparing the effect of the solvent used to prepare the dye solution. It was found that using an ACN:*t*-BuOH mixture resulted in higher absorbance by the substrate with anchored dye molecules. This could indicate the anchoring of different numbers of dye molecules which definitely affects the final PV performance of the solar cells. In general, shifts of

absorption band maxima ( $\lambda_{\max}$ ) towards longer wavelengths were observed for all dyes dissolved in ACN:*t*-BuOH compared to DMF. However, in the case of photoanodes prepared with chloroform, it was found that for **PTZ-1** and **PTZ-2**, the largest bathochromic shift  $\lambda_{\max}$  was observed with respect to DMF and ACN:*t*-BuOH. The absorption maximum of the photoanode with **PTZ-3** (464 nm) underwent a bathochromic shift compared to the electrode prepared with DMF (437 nm), but a hypochromic

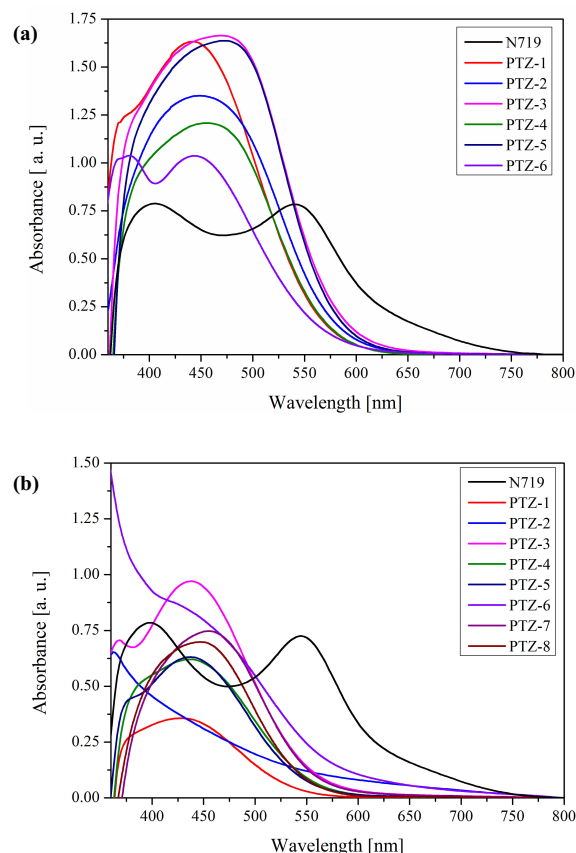


Fig. 2. UV-Vis absorption spectra of the studied TiO<sub>2</sub>-anchored dyes from a solution of (a) DMF and (b) ACN:*t*-BuOH.

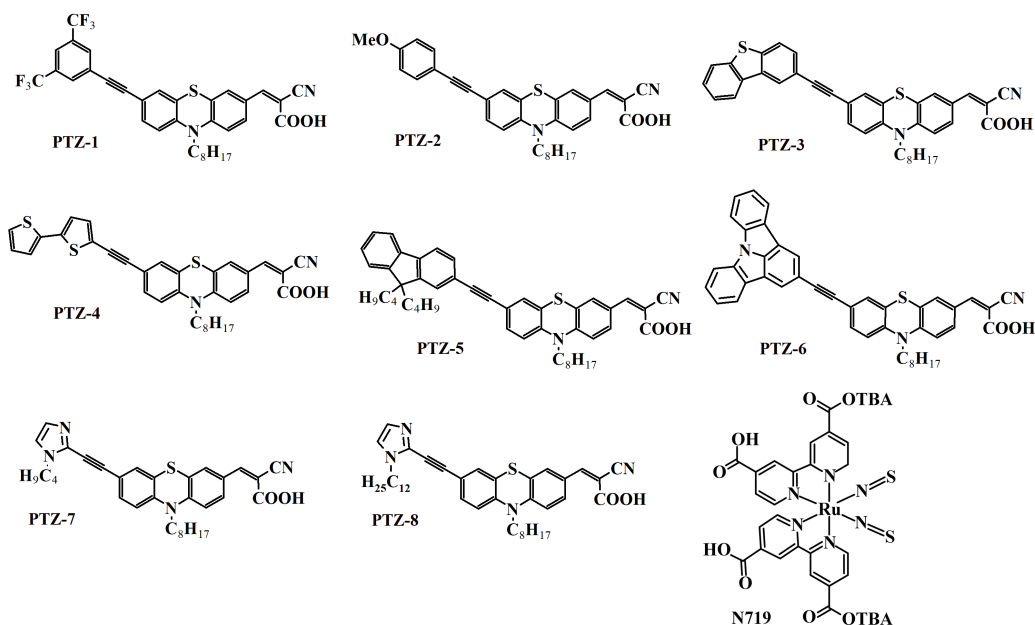


Fig. 1. Chemical structures of phenothiazine derivatives and N719.

shift compared to the photoanode prepared with ACN:t-BuOH (469 nm). The hypsochromic shifts  $\lambda_{\max}$  compared to the corresponding photoanodes were observed for **PTZ-4** and **PTZ-5** ( $\text{CHCl}_3$ ) anchored in  $\text{TiO}_2$ . Similar to the increase in absorbance, this may have had a definite effect on the devices short-circuit current density ( $J_{\text{sc}}$ ) values. **PTZ-3** and **PTZ-5**, containing dibenzothiophene and dibutylfluorene substituents, respectively, were found to have the highest absorbance. Furthermore,  $\lambda_{\max}$  showed the greatest shift towards longer wavelengths, except for the photoanode with **PTZ-5** ( $\text{CHCl}_3$ ).

### 3.2. Electrochemical properties

In addition to the optical properties, the position of the HOMO and LUMO levels (Fig. 3) of the dyes is very important. In the case of the dye **PTZ-6**, the LUMO level was determined using the optical energy gap (1240/ $\lambda$ ). The studied compounds showed both quasi-reversible (**PTZ-1**, **PTZ-4**, and **PTZ-5**), as well as irreversible (**PTZ-2**, **PTZ-3**, **PTZ-6**, **PTZ-7**, and **PTZ-8**) oxidation processes. In the case of reduction, most of the dyes were characterised by an irreversible process, and in the case of **PTZ-6**, no irreversible process was observed during the measurements.

Analysing the data shown in Fig. 3, it was found that each of the dyes investigated fulfilled the conditions of matching the energy levels of HOMO and LUMO to the conduction band of  $\text{TiO}_2$  and the redox potential of the electrolyte. The LUMO orbitals were determined in the

range from  $-3.88$  eV to  $-2.94$  eV. The position of the LUMO levels for the phenothiazine derivatives in question mainly depends on the chemical structure of the substituent at position 3. Considering the most favourable alignment of LUMO levels concerning the  $\text{TiO}_2$  conduction band, phenothiazine derivatives containing dibenzothiophene (**PTZ-3**), bitiophene (**PTZ-4**), and dibutylfluorene (**PTZ-5**) substituents stood out. These substituents resulted in a lower LUMO than the other studied phenothiazine derivatives. In addition, the use of a dibutylfluorene substituent (**PTZ-5**) resulted in the lowest energy gap, with a value of 1.69 eV, while the presence of a bis(trifluoromethylphenyl) group (**PTZ-1**) increased the  $E_g$  value to 2.54 eV. The localisation of the LUMO orbitals of the **PTZ-3**, **PTZ-4**, and **PTZ-5** dyes was more favourable and could ensure efficient electron injection into  $\text{TiO}_2$  and reduce competing processes. Comparing the HOMO level alignment of the phenothiazine derivatives, no significant differences were observed (from  $-5.49$  eV to  $-5.40$  eV), and all of the determined values were lower than the redox potential of the electrolyte iodide ( $-4.8$  eV). In Refs. 35 and 36, the relationship between the energy gap value and the performance of the DSSC cell was observed. It was found that as the  $E_g$  value decreased, the PCE value of the devices increased. Based on the cited works, it could be concluded that the use of **PTZ-3**, **PTZ-4**, and **PTZ-5** dyes should determine high energy conversion efficiencies. However, it should be borne in mind that the efficiency of the cell is also affected by other properties of the dye.

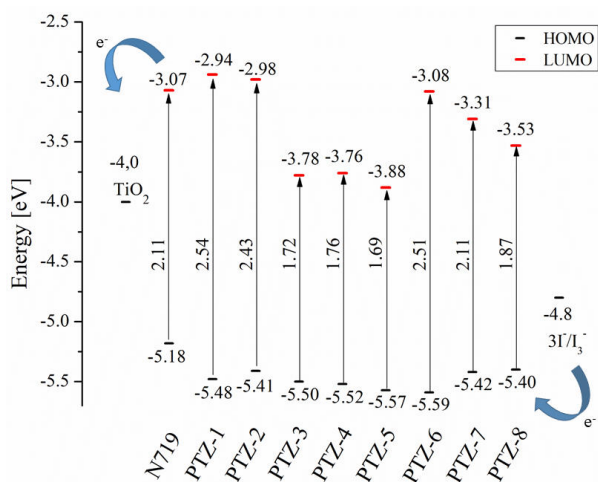


Fig. 3. Energy diagram of phenothiazine derivatives with  $\text{TiO}_2$  conductivity band and electrolyte redox potential [37].

### 3.3. Photoanodes morphology

The next step of the ongoing research was to determine the morphology of photoanodes with anchored phenothiazine derivative molecules. The RMS value was determined from AFM measurements and compared with an anode containing anchored N719 molecules and with  $\text{TiO}_2$  on FTO without dye. The photoanodes with adsorbed dye molecules showed RMS values in the 18–27 nm range. No significant differences due to the chemical structure of the dye were observed, however, it was noted that all phenothiazine derivatives tested filled the pores of  $\text{TiO}_2$  very well, as indicated by a significant reduction in RMS from around 75 nm ( $\text{TiO}_2$  without dye). A slight effect of the solvent used on the surface roughness was observed, as the differences were in the 1–5 nm range when DMF and chloroform were used for ACN:t-BuOH. Figure 4 shows example AFM images of the fabricated anodes.

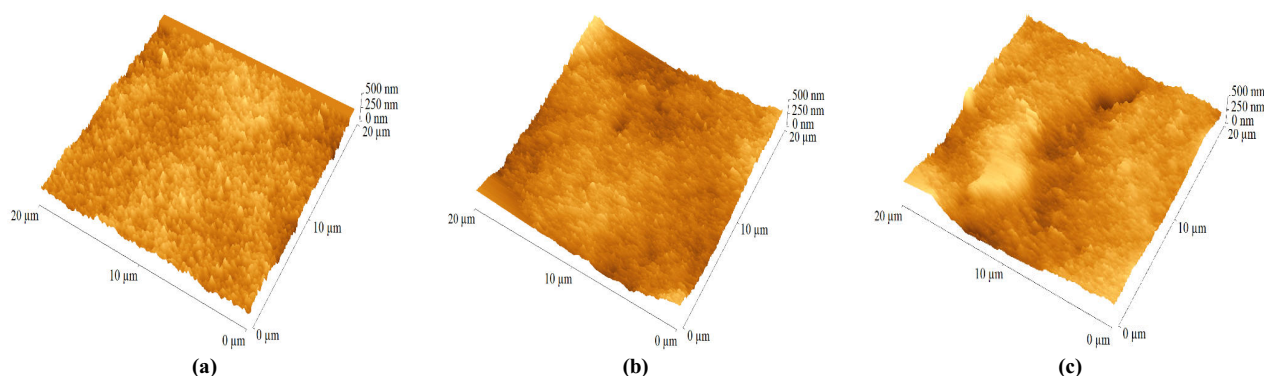


Fig. 4. AFM images of (a)  $\text{TiO}_2$  substrate without adsorbed dyes molecules, (b)  $\text{TiO}_2$ @N719, and (c)  $\text{TiO}_2$ @PTZ-3.



### 3.4. Photovoltaic performance.

The final step in this part of the study was the preparation of DSSCs with a glass/FTO/TiO<sub>2</sub>@dye/EL-HSE/Pt/FTO/glass structure. The dye concentration in each case was  $3 \cdot 10^{-4}$  M. Based on the recorded current-voltage curves (Fig. 5), photovoltaic parameters such as open circuit voltage ( $V_{oc}$ ), short circuit current density ( $J_{sc}$ ), fill factor (FF) and PCE were determined (Table 1).

Three solvents were used: DMF because all the phenothiazine derivatives tested dissolved well in it, ACN:t-BuOH mixture because it provided higher energy conversion efficiencies in the case of N719, and chloroform since there is little information in the literature regarding the use of this solvent for the preparation of photoanodes. In the case of compounds **PTZ-7** and **PTZ-8**, the PV parameters of the devices were not determined, except for the cells with the photoanode prepared in DMF, as these compounds showed too poor solubility in other solvents. After analysis of the results obtained, a definite effect of the solvent used on the PV performance of the fabricated cells was found. The same situation was for **PTZ-6** in chloroform. Using a mixture of ACN:t-BuOH in place of DMF, it was observed that there was an increase in both  $V_{oc}$  and  $J_{sc}$  each time. The changes in  $V_{oc}$  were in the range of 59–93 mV. The largest increase in  $V_{oc}$  with solvent change was recorded for **PTZ-4** (with a bitiophene substituent). The largest differences were observed for  $J_{sc}$  which reached as high as  $12.49 \text{ mA cm}^{-2}$  for the phenothiazine derivative

**Table 1.**  
Photovoltaic parameters of DSSCs sensitized with phenothiazine derivatives.

Dye	Solvent	$V_{oc}$ [mV]	$J_{sc}$ [ $\text{mA cm}^{-2}$ ]	FF	PCE [%]
<b>N719</b>	DMF	664	13.73	0.56	5.35
	ACN:t-BuOH	723	20.19	0.42	6.29
	CHCl <sub>3</sub>	–	–	–	–
<b>PTZ-1</b>	DMF	667	2.95	0.60	1.55
	ACN:t-BuOH	720	15.44	0.54	6.16
	CHCl <sub>3</sub>	730	15.38	0.45	5.03
<b>PTZ-2</b>	DMF	700	6.34	0.59	2.63
	ACN:t-BuOH	757	14.76	0.57	6.40
	CHCl <sub>3</sub>	759	16.74	0.49	6.21
<b>PTZ-3</b>	DMF	691	7.54	0.57	2.94
	ACN:t-BuOH	778	17.87	0.51	7.26
	CHCl <sub>3</sub>	700	17.96	0.48	6.22
<b>PTZ-4</b>	DMF	652	6.89	0.59	2.71
	ACN:t-BuOH	745	14.87	0.50	6.14
	CHCl <sub>3</sub>	631	11.87	0.54	4.22
<b>PTZ-5</b>	DMF	724	8.78	0.65	4.19
	ACN:t-BuOH	792	17.85	0.49	7.09
	CHCl <sub>3</sub>	703	12.08	0.56	4.80
<b>PTZ-6</b>	DMF	647	6.60	0.64	2.87
	ACN:t-BuOH	715	11.58	0.62	5.23
	CHCl <sub>3</sub>	–	–	–	–
<b>PTZ-7</b>	DMF	692	6.81	0.61	2.96
	ACN:t-BuOH	–	–	–	–
	CHCl <sub>3</sub>	–	–	–	–
<b>PTZ-8</b>	DMF	699	9.22	0.63	4.19
	ACN:t-BuOH	–	–	–	–
	CHCl <sub>3</sub>	–	–	–	–

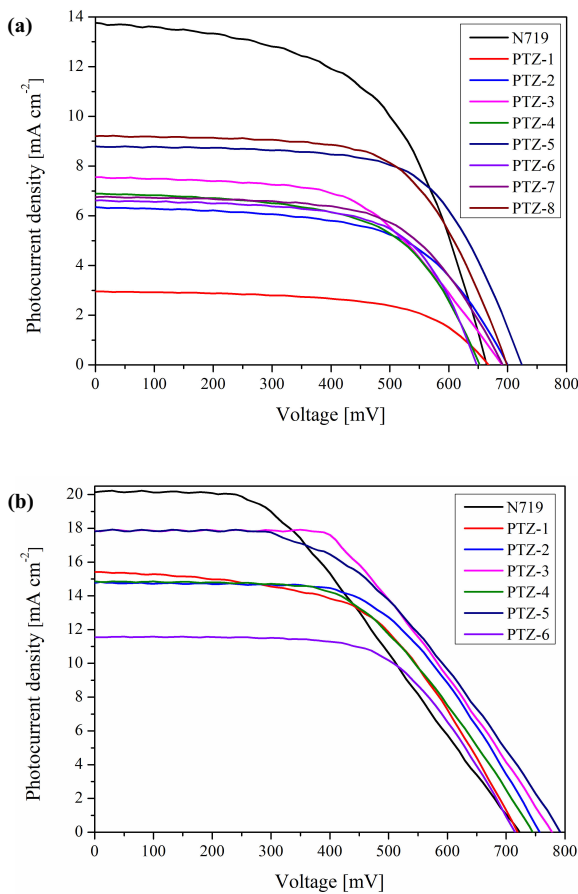


**Fig. 5.** Current-voltage curves of devices containing phenothiazine derivatives (a) photoanodes prepared in DMF and (b) in a mixture of ACN:t-BuOH.

with a bis(trifluoromethylphenyl) substituent (**PTZ-1**). A decrease in FF values in the range of 0.02–0.16 was observed in each case when changing the solvent from DMF to ACN:t-BuOH. Using chloroform, devices containing the dyes **PTZ-1**, **PTZ-2**, and **PTZ-3** showed the lowest FF compared to other solvents used. The determined PV parameters of the prepared devices allowed the calculation of the light-to-electricity conversion efficiency. The first thing highlighted was significant efficiency differences depending on the solvent used. This effect was clearly observed for **PTZ-1** and **PTZ-3** for which the PCE values increased by nearly 300% and 150%, respectively, when using an ACN:t-BuOH mixture instead of DMF. This

is most likely related to the number of dye molecules anchored to TiO<sub>2</sub>. These studies were carried out using the dye N719 for different solvents and confirmed that, depending on the solvent used to prepare the dye solution, a different number of molecules of the compound anchor to TiO<sub>2</sub>. The number of anchored dye molecules directly influences the absorption properties of the photoanode and, in the long term, the photocurrent density generated. Based on Ref. 27, it was found that the use of the ACN:t-BuOH mixture resulted in the highest number of dye molecules being anchored to TiO<sub>2</sub>, and thus the highest  $J_{sc}$  values were obtained, which was also confirmed in the studies described in this work. Based on the data in Table 1, the highest energy conversion efficiency was provided by using the dibenzothiophene-substituted phenothiazine derivative (PTZ-3) which was 7.26%.

Since the use of the PTZ-3 dye allowed the device to achieve the highest efficiency, attempts were made to modify the cell by using a TiO<sub>2</sub> BL and a co-adsorbent which was CDCA added at a concentration of 10 mM to the dye solution. Solar cells with a glass/FTO/BL/TiO<sub>2</sub>@dye/s:CDCA/EL-HSE/Pt/FTO/glass structure were prepared. The PV parameters of DSSCs sensitized with PTZ-3 with a modified structure determined from the obtained current-voltage curves (Fig. 6) are summarized in Table 2.

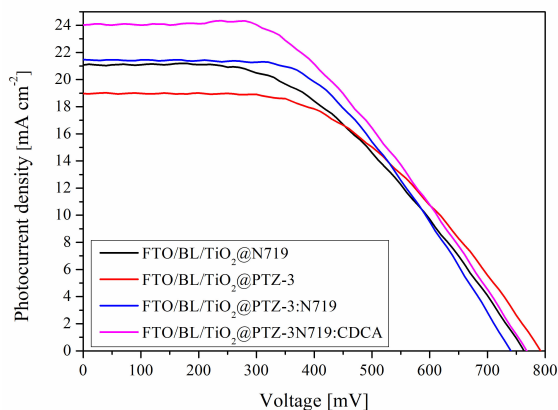


Fig. 6. Photocurrent-voltage curves of modified DSSCs sensitized with PTZ-3.

**Table 2.**  
Photovoltaic performance of the modified DSSCs sensitized with PTZ-3 and N719.

Structure of photoanode	$V_{oc}$ [mV]	$J_{sc}$ [mA cm <sup>-2</sup> ]	FF	PCE [%]
FTO/BL/TiO <sub>2</sub> @N719	762	21.08	0.47	7.49
FTO/BL/TiO <sub>2</sub> @PTZ-3	792	19.02	0.50	7.62
FTO/BL/TiO <sub>2</sub> @PTZ-3:N719	740	21.45	0.51	8.04
FTO/BL/TiO <sub>2</sub> @PTZ-3:N719:CDCA	768	24.05	0.46	8.50

Analysing the effect of BL application on the PV parameters of cells containing N719 and PTZ-3 dyes, an increase in  $V_{oc}$  and  $J_{sc}$  was found in both cases. The effect of obtaining higher values for these parameters was to

improve the PCE of the cells by nearly 20% and 5% for N719 and PTZ-3, respectively. The use of the dye mixture resulted in an increase in  $J_{sc}$  which was most likely due to the expansion of the absorption range of the photoanode and thus the conversion of more photons to electrons. With a higher  $J_{sc}$ , an efficiency of 8.04% was achieved. A further modification with CDCA added resulted in a cell efficiency of 8.50%. This was made possible by an increase in  $V_{oc}$  of 28 mV and 2.60 mA cm<sup>-2</sup>, however, there was also a decrease of 0.05 in FF at the same time.

#### 4. Conclusions

The study showed a significant effect of the solvent used to prepare the dye solutions to produce the photoanode. The most beneficial was found to be the use of an ACN:t-BuOH mixture (1:1), which translated into the highest yields (7.26% for PTZ-3). Further modifications, i.e., the use of a TiO<sub>2</sub> BL, a CDCA additive, and a dye mixture (PTZ-3:N719), allowed the device performance to be improved by more than 35% relative to N719, thus achieving a PCE of 8.50%. The use of the dye mixture is important in terms of reducing the amount of commercial compound N719 used which reduces the cost of preparing the solar cell, and thus the ratio of the cost of the device to the amount of electricity it generates becomes more favourable.

#### Acknowledgements

Part of the research was co-financed by the NCN OPUS-21 project no. 2021/41/B/ST5/03221.

#### Authors' statement

Research concept and design, P.G.; collection and/or assembly of data, P.G.; data analysis and interpretation, P.G. E.S-B.; writing the article, E.S-B., P.G., and A.S.; critical revision of the article, E.S-B.; final approval of article, M.Ł., E.S-B., A.S., and P.G.

#### References

- [1] Griep, M.H. *et al.* Development of thin-film dye-sensitized photoactive materials on ultra high molecular weight polyethylene (First-year Report). Army Research Laboratory. <https://www.govinfo.gov/content/pkg/GOVPUB-D101-PURL-gpo126384/pdf/GOVPUB-D101-PURL-gpo126384.pdf> (2012).
- [2] Solak, F. K. & Irmak, E. Advances in organic photovoltaic cells: a comprehensive review of materials, technologies, and performance. *RSC Adv.* **13**, 12244–12269 (2023). <https://doi.org/10.1039/d3ra01454a>
- [3] Yahya, M., Bouziani, A., Ocak, C., Seferoğlu, Z. & Sillanpää, M. Organic/metal-organic photosensitizers for dye-sensitized solar cells (DSSC): Recent developments, new trends, and future perceptions. *Dyes Pigments* **192**, 109227 (2021). <https://doi.org/10.1016/j.dyepig.2021.109227>
- [4] Kakiage, K. *et al.* Highly-efficient dye-sensitized solar cells with collaborative sensitization by silyl-anchor and carboxy-anchor dyes. *Chem. Commun.* **51**, 15894–15897 (2015). <https://doi.org/10.1039/c5cc06759f>
- [5] Ye, M. *et al.* Recent advances in dye-sensitized solar cells: From photoanodes, sensitizers and electrolytes to counter electrodes. *Mater. Today* **18**, 155–162 (2015). <https://doi.org/10.1016/j.mattod.2014.09.001>

- [6] Song, L., Du, P., Xiong, J., Ko, F. & Cui, C. Efficiency enhancement of dye-sensitized solar cells by optimization of electrospun ZnO nanowire/nanoparticle hybrid photoanode and combined modification. *Electrochim. Acta.* **163**, 330–337 (2015). <https://doi.org/10.1016/j.electacta.2015.02.093>
- [7] Prakash, P. & Janarthanan, B. Review on the progress of light harvesting natural pigments as DSSC sensitizers with high potency. *Inorg. Chem. Commun.* **152**, 110638 (2023). <https://doi.org/10.1016/j.inoche.2023.110638>
- [8] Kim, M. H. & Kwon, Y. U. Semiconductor CdO as a blocking layer material on DSSC electrode: Mechanism and application. *J. Phys. Chem. C* **113**, 17176–17182 (2009). <https://doi.org/10.1021/jp904206a>
- [9] Nguyen, D.-T., Kurokawa, Y. & Taguchi, K. Enhancing DSSC photoanode performance by using Ni-doped TiO<sub>2</sub> to fabricate scattering layers. *J. Electron. Mater.* **49**, 2578–2583 (2020). <https://doi.org/10.1007/s11664-020-07965-7>
- [10] Gnida, P. *et al.* Impact of blocking layer on DSSC performance based on new dye-indolo[3,2,1-jk]carbazole derivative and N719. *Dyes Pigments* **200**, 110166 (2022). <https://doi.org/10.1016/j.dyepig.2022.110166>
- [11] Sibiński, M. *et al.* Impact of blocking layers based on TiO<sub>2</sub> and ZnO prepared via direct current reactive magnetron sputtering on DSSC solar cells. *Sci. Rep.* **14**, 1–11 (2024). <https://doi.org/10.1038/s41598-024-61512-6>
- [12] Gnida, P. *et al.* Impact of TiO<sub>2</sub> nanostructures on dye-sensitized solar cells performance. *Materials (Basel)*. **14**, 13–15 (2021). <https://doi.org/10.3390/ma14071633>
- [13] Zakir, O. *et al.* A review on TiO<sub>2</sub> nanotubes: synthesis strategies, modifications, and applications. *J. Solid State Electrochem.* **27**, 2289–2307 (2023). <https://doi.org/10.1007/s10008-023-05538-2>
- [14] Elzarka, A., Liu, N., Hwang, I., Kamal, M. & Schmuki, P. Large-diameter TiO<sub>2</sub> nanotubes enable wall engineering with conformal hierarchical decoration and blocking layers for enhanced efficiency in dye-sensitized solar cells (DSSC). *Chem. Eur. J.* **23**, 12995–12999 (2017). <https://doi.org/10.1002/chem.201702434>
- [15] Sasidharan, S. *et al.* Fine tuning of compact ZnO blocking layers for enhanced photovoltaic performance in ZnO based DSSCs: a detailed insight using  $\beta$  recombination, EIS, OCVD and IMVS techniques. *New J. Chem.* **41**, 1007–1016 (2017). <https://doi.org/10.1039/c6nj03098j>
- [16] Duong, T.-T., Choi, H.-J., He, Q.-J., Le, A.-T. & Yoon, S.-G. Enhancing the efficiency of dye sensitized solar cells with an SnO<sub>2</sub> blocking layer grown by nanocluster deposition. *J. Alloys Compd.* **561**, 206–210 (2013). <https://doi.org/10.1016/j.jallcom.2013.01.188>
- [17] Cho, T.-Y., Yoon, S.-G., Sekhon, S.-S., Kang, M.-G. & Han, C.-H. The effect of a sol-gel formed TiO<sub>2</sub> blocking layer on the efficiency of dye-sensitized solar cells. *Bull. Korean Chem. Soc.* **32**, 3629–3633 (2011). <https://doi.org/10.5012/bkcs.2011.32.10.3629>
- [18] Park, N.-G. *et al.* Morphological and photoelectrochemical characterization of core-shell nanoparticle films for dye-sensitized solar cells: Zn-O type shell on SnO<sub>2</sub> and TiO<sub>2</sub> cores. *Langmuir* **20**, 4246–4253 (2004). <https://doi.org/10.1021/la036122x>
- [19] Kay, A. & Grätzel, M. Dye-sensitized core-shell nanocrystals: Improved efficiency of mesoporous tin oxide electrodes coated with a thin layer of an insulating oxide. *Chem. Mater.* **14**, 2930–2935 (2002). <https://doi.org/10.1021/cm0115968>
- [20] Prakash, G. & Subramanian, K. Interaction of pyridine  $\pi$ -bridge-based poly(methacrylate) dyes for the fabrication of dye-sensitized solar cells with the influence of different strength phenothiazine, fluorene and anthracene sensitizers as donor units with new anchoring mode. *New J. Chem.* **42**, 17939–17949 (2018). <https://doi.org/10.1039/c8nj04068k>
- [21] Lee, K.-M. *et al.* Effects of co-adsorbate and additive on the performance of dye-sensitized solar cells: A photophysical study. *Sol. Energy Mater. Sol. Cells* **91**, 1426–1431 (2007). <https://doi.org/10.1016/j.solmat.2007.03.009>
- [22] Slodek, A. *et al.* New benzo[h]quinolin-10-ol derivatives as co-sensitizers for DSSCs. *Materials (Basel)* **14**, 3386 (2021). <https://doi.org/10.3390/ma14123386>
- [23] Feng, Q., Wang, H., Zhou, G. & Wang, Z.-S. Effect of deoxycholic acid on performance of dye-sensitized solar cell based on black dye. *Front. Optoelectron.* **4**, 80–86 (2011). <https://doi.org/10.1007/s12200-011-0209-y>
- [24] Elangovan, K. *et al.* Simple phenothiazine-based sensitizers for dye-sensitized solar cells: Impact of different electron-donors on their photovoltaic performances. *J. Mater. Sci. Mater. Electron.* **35**, 1154 (2024). <https://doi.org/10.1007/s10854-024-12870-4>
- [25] Dhivya, K. S., Senthilkumar, C., Karthika, K. & Srinivasan, P. Structural, electrical, optical, and DFT studies of phenothiazine-based D- $\pi$ -A frameworks for dye-sensitized solar cell applications. *Struct. Chem.* **24**, (2024). <https://doi.org/10.1007/s11224-024-02327-z>
- [26] Sekkat, Y. *et al.* A theoretical study on the role of the  $\pi$ -spacer in the thoughtful design of good light-absorbing dyes with phenothiazine for efficient dye-sensitized solar cells (DSSCs). *J. Mol. Model.* **30**, 5 (2024). <https://doi.org/10.1007/s00894-023-05783-2>
- [27] Gnida, P., Libera, M., Pająk, A. & Schab-Balcerzak, E. Examination of the effect of selected factors on the photovoltaic response of dye-sensitized solar cells. *Energy Fuels* **34**, 14344–14355 (2020). <https://doi.org/10.1021/acs.energyfuels.0c02188>
- [28] Luo, J. *et al.* Co-sensitization of dithiafulvenyl-phenothiazine based organic dyes with N719 for efficient dye-sensitized solar cells. *Electrochim. Acta* **211**, 364–374 (2016). <https://doi.org/10.1016/j.electacta.2016.05.175>
- [29] Wang, X. Enhanced performance of dye-sensitized solar cells based on a dual anchored diphenylpyranylidene dye and N719 co-sensitization. *J. Mol. Struct.* **1206**, 127694 (2020). <https://doi.org/10.1016/j.molstruc.2020.127694>
- [30] Cole, J. M., Pepe, G., Al Bahri, O. K. & Cooper, B. C. Cosensitization in dye-sensitized solar cells. *Chem. Rev.* **119**, 7279–7327 (2019). <https://doi.org/10.1021/acs.chemrev.8b00632>
- [31] Job, F., Mathew, S., Meyer, T. & Narbey, S. Studies on the performance and stability of dye-sensitized solar cells based on the co-sensitization of N719 and RK1 dye-sensitizers. *Optik (Stuttgart)* **292**, 171215 (2023). <https://doi.org/10.1016/j.ijleo.2023.171215>
- [32] Slodek, A. *et al.* Investigations of new phenothiazine-based compounds for dye-sensitized solar cells with theoretical insight. *Materials (Basel)* **13**, 2292 (2020). <https://doi.org/10.3390/ma13102292>
- [33] Slodek, A. *et al.* Dyes based on the D/A-acetylene linker-phenothiazine system for developing efficient dye-sensitized solar cells. *J. Mater. Chem. C* **7**, 5830–5840 (2019). <https://doi.org/10.1039/c9tc01727e>
- [34] Zimosz, S. *et al.* New D- $\pi$ -D- $\pi$ -A systems based on phenothiazine derivatives with imidazole structures for photovoltaics. *J. Phys. Chem. C* **126**, 8986–8999 (2022). <https://doi.org/10.1021/acs.jpcc.2c01697>
- [35] Wu, H. *et al.* Low-energy-gap organic photosensitizers with phenalenothiophene and benzoindothiophene as primary electron-donors for durable dye-sensitized solar cells. *J. Power Sources* **451**, 227748 (2020). <https://doi.org/10.1016/j.jpowsour.2020.227748>
- [36] Ahmed, M. I. Effect of changing solvents on absorbance, optical energy gaps and efficiency for zinc oxide and rose bengal dye solar cells. *Int. J. Innov. Sci. Eng. Technol.* **6**, 77–85 (2019).
- [37] Consiglio, G., Gorczyński, A., Petralia, S. & Forte, G. Predicting the dye-sensitized solar cell performance of novel linear carbon chain-based dyes: insights from DFT simulations. *Dalton Trans.* **52**, 15995–16004, (2023). <https://doi.org/10.1039/d3dt01856c>